2D numerical model for heat transfer on a laser deposited high entropy alloy baseplate using comsol multiphysics.

Materials Today: Proceedings 50 (2022) 2541–2546

Contents lists available at ScienceDirect

Materials Today: Proceedings

journal homepage: www.elsevier.com/locate/matpr

2D numerical model for heat transfer on a laser deposited high entropy alloy baseplate using Comsol Multiphysics

M. Dada [a,*], P. Popoola [a], N. Mathe [b], S. Adeosun [c], O. Aramide [a]

[a] Chemical, Metallurgical and Materials Engineering, Tshwane University of Technology, Pretoria 0183, South Africa
[b] Council for Scientific and Industrial Research, 0184, South Africa
[c] Metallurgical and Materials Engineering, University of Lagos, Akoka 100213, Nigeria

ARTICLE INFO

Article history:
Received 18 September 2021
Received in revised form 19 October 2021
Accepted 2 December 2021
Available online 27 December 2021

Keywords:
Comsol multiphysics
High entropy alloys
Steel baseplate
Laser deposition

ABSTRACT

In an optimization study, cracks were observed in the microstructures of laser-deposited HEAs on a steel baseplate from residual stresses, thus, the optimization of crack-free microstructures was achieved by the optimization of the laser parameters by baseplate preheating attributed to the lowering of the thermal gradients of the deposition process. This study reports the finite element analysis on the temperature distribution by the moving laser modelled to achieve process optimization with the necessary boundary conditions. Simulation has been reported as a facilitating tool in predicting the behaviour of materials during process optimization. Comsol Multiphysics 4.4, was used to create a 2D transient heat transfer time-dependent model to simulate the temperature distribution and the laser heating of the A301 steel baseplate surface and determine the effect of temperature on the optimization process of the alloys. Gaussian profiles were used as the heat source distributed per time. The results are presented in terms of thermal fields and Gaussian temperature profiles. Which show the temperature distribution that occurred in the steel baseplate during fabrication and the high cooling rate of the laser additive manufacturing technique restricted thermal stresses, improving adhesion and facilitating the optimization process.

Selection and peer-review under responsibility of the scientific committee of the 2nd International Conference on Functional Material, Manufacturing and Performances

1. Introduction

Metal laser deposition is a process where metal powder is melted by a laser to fabricate fully dense parts [1]. This characteristic feature gives the technique an unlimited possibility in the production of tools, structural parts, and cavities [2]. Nonetheless, one major challenge of the laser-deposition system is the development of thermal stresses, attributed to the increased amount of thermal gradients during deposition. In a previous study [3,4], defects were observed in the microstructures of the high entropy alloy (HEA) coatings fabricated on a steel base plate. Reports in the literature suggest that increasing the temperature of the baseplate via preheating temperature reduces the temperature gradients [5]. In recent times, modelling and simulation of metal laser deposition processes are used as a non-destructive time control tool to avoid further trial-and-errors. Therefore, computational modelling was applied in investigating the heat transfer mechanisms on the HEA steel baseplate when the laser is moving with constant power and a stationary laser with constant power and pulsed power [6]. Bianco et al. [7] explored the numerical analysis on the transient 3D temperature distribution in a semi-infinite solid exposed by a Gaussian beam. The authors presented the results in thermal fields and temperature profiles, which showed that the material reached a quasi-steady state and the convective heat transfer on the surface of the material, had the most influence on the optimization process. Htin Linn et al. [8] modelled the parameter optimization of the heating process of metals using Comsol Multiphysics 5.3a to solve the problems associated with the laser heating process and the resulting thermal properties of complex materials. The laser processing parameters, such as the temperature and focal point of the laser, surface emissivity, the laser speed and power were controlled using the model. The results showed that the scanning speed and power had the most influence on the laser heating process, which helps understand the parameter setting needing adjustment during deposition for improved properties and mate-

* Corresponding author.
E-mail address: dadadupeola@gmail.com (M. Dada).

https://doi.org/10.1016/j.matpr.2021.12.068

Selection and peer-review under responsibility of the scientific committee of the 2nd International Conference on Functional Material, Manufacturing and Performances

rial effectiveness. Darif et al. [9] examined the numerical simulation of the nanosecond laser annealing of silicon using a two-dimensional heat conduction Comsol Multiphysics model to investigate the significance of laser thermal processing and its properties in complex materials. The results were presented in temperature versus depth and surface temperature versus energy density and time profiles. Heat conduction was used as the governing equation to determine the heat source distributed per time and to understand the transport phenomenon of silicon during the laser process. The results showed that silicon had several values of the melting duration and melting pool under the treatment of the pulsed laser. The authors recommended that, to refine the laser threshold, the study of the melting kinetics of Silicon should be done in the range of 800–1100 mJ/cm^2. Caiazzo et al. [10] explored the simulation of laser heating of non-penetrative bead-on-plate welds of an aluminum alloy using Comsol Multiphysics. The results showed that the model is moderately capable of predicting the temperature of the laser heating process and producing the appropriate melt pool for the additive manufacturing process. An average error of 4% shows that the model can predict the depth of the fusion zone. Parekh et al. [11] developed a 2D simulation of the laser cladding process using Comsol Multiphysics to understand the influence of the laser processing parameters on the clad geometry. The modelling was achieved by varying one parameter while other parameters are kept constant to give a clear distinction of which parameter such as the laser speed and power, the beam diameter and the mass flow rate had the most influence on the optimization process. The results showed that the laser power had a significant influence on the clad geometry compared to other parameters. An increase in the laser power increased the clad temperature, height and dilution. Morville et al. [12] developed a 3D model using Comsol Multiphysics to predict the coaxial powder flow process during laser deposition of metals to examine the effect of the laser parameters on the surface finishing of the coatings produced via additive manufacturing. The results showed that the substrate positioning under the melt pool significantly influences the clad surface finish. The authors detailed that the surface finishing of clads are improved when the surface of the substrate is situated at the focus plane of the powder stream. Therefore, the location of the powder focus plane must correspond with the position of the substrate for optimum deposition. Cao et al. [13] scrutinized the temperature field of the heat transfer process to determine the effect of the heating temperature on the substrate. The authors stated that the temperature gradient distribution is influenced by the heating temperature, therefore; optimization of the heating temperature is necessary for fusion of the clad on the substrate and fusion between clad layers for better placement efficiency. Farotade et al. [6] used a 3D computation analysis via Comsol Multiphysics to analyze the heat transfer on a titanium alloy substrate during laser deposition. The results showed that the laser process parameters such as the scanning speed, beam spot size and laser power had a major influence on the temperature distribution. Phase changes were also observed when the temperature increased thus indicating that the model is suitable for predicting the phase changes that occur during the laser-deposition process at several coordinates of the subsurface of the substrate. From, the literature review, Comsol Multiphysics shows great potential in the optimization of the metal laser deposition process. However, the computational analysis of the heat transfer of a HEA baseplate during laser deposition is limited in the literature [6]. In the present study, Comsol Multiphysics was used to examine the heat transfer mechanism on the steel baseplate during laser deposition of HEAs.

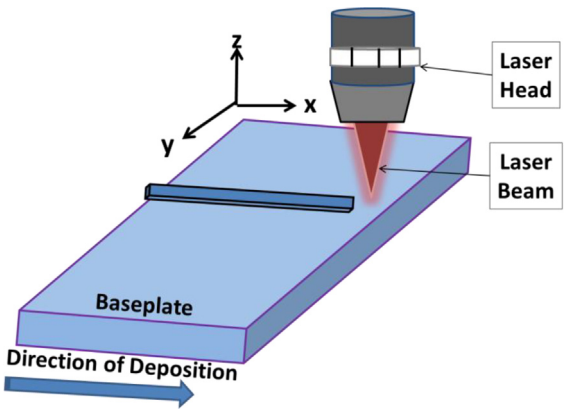

Fig. 1. Schematic of the Laser-deposition Process [6].

2. Computational analysis

A schematic of the laser deposition process is presented in Fig. 1. Deposition of the HEA coatings was made on a 40 mm × 4 mm baseplate shown in Fig. 2. The HEAs metal powder was fed into powder hoppers, which inject the metal powder through coaxial nozzles into the molten pool created by the laser beam. At a laser scanning speed between 8 mm/s and 12 mm/s, the HEA melt deposited on the steel baseplate solidifies quickly, forming a track on solidification. The process is repeated, building the HEA coating layer-by-layer on the baseplate using a 3 kW ytterbium laser-deposition system with a fiber laser as the heat source. The melt pool comprises the middle inlet, where argon gas directs the HEA powder into the molten pool. The deposition process was done in a continuous wave mode by varying the laser scanning speed and power, while other parameters remained constant. After fabrication, cracks were observed in the microstructures of the alloys from residual stresses. Simulation and modelling have been reported as facilitating tools in predicting the behaviour of materials during process optimization. Therefore, Comsol Multiphysics was used to create a 2D transient heat transfer time-dependent model to simulate the laser heating of the A301 steel baseplate surface and determine the effect of temperature on the optimization process of the alloys [10]. The global expression used in the Simulation via Comsol Multiphysics is shown in Table 1. Thus, experimental investigations after simulation verified the optimum temperature for the fabrication of HEAs on a steel base plate was between 1200 °C and 1600 °C where crack-free microstructures were achieved by baseplate preheating at 400 °C attributed to the lowering of the thermal gradients of the deposition process. The HEA, after preheating the baseplate, also had good adhesion and metallurgical bonding with the plates. The heat transfer module was used to indicate the phases within the baseplate, which drives the behavioral properties of the steel during deposition. Finite element analysis of the moving laser with constant power and stationary laser with constant power and pulsed power on the plates per time were all investigated with the laser heat source distributed in time with Gaussian profiles. The results showed the temperature changes that occurred in the steel baseplate during fabrication and the high cooling rate of the laser additive manufacturing technique prevented phase changes on the baseplate depth, which helped improve adhesion and facilitate the optimization process.

2.1. Assumptions

The assumptions made in the development of this model are:

Table 1
Global expressions used in the Simulation via Comsol Multiphysics.

Name	Expression	Description
S_Laser	1600 [W]	Laser Power
S_ScanSpeed	10 [mm/s]	Scan Speed
Width	40 [mm]	Substrate Width
Height	4 [mm]	Substrate Height
BeamDiameter	2 [mm]	Beam Diameter
StandardDeviation	BeamDiameter/4	Standard Deviation
stop	Width/ S_ScanSpeed	Single pass duration
x0	0.5 [mm]	Beam Position x-axis
y0	0 [mm]	Beam Position y-axis
A1	pi/4* (BeamDiameter)^2	Area
B1	S_Laser/A1	Beam Intensity
sigx	0.3 [mm]	Pulse × standard deviation
sigy	0.5 [mm]	Pulse y standard deviation
Rc	0.05	Reflection coefficient
Ac	0.5 [1/cm]	Absorbtion coefficient
S_Rotation	15 [rpm]	Rotational Speed
S_emissivity	0.8	Surface emissivity
Diagonal	56.57 [mm]	Diagonal of substrate surface
S_Radius	Diagonal/2 [in.]	Circumcircle radius of Substrate Surface
S_Area	0.0016 [m^2]	Area of substrate surface
Laser_time	10 [s]	Time for laser to move back and forth

- The geometry only models the A301 steel and its properties are assumed to be constant.
- All other boundaries are kept constant except for the boundaries on the top surface
- The laser beam's electromagnetic properties are not stimulated; therefore the effect of its wavelength is not modelled. While changing x0 and y0 can shift the beam's center while the astigmatism and the width of the beam can be controlled through $\sigma_x\sigma_y$.

3. Governing equations and boundary conditions

3.1. Heat equations

The surface of the steel baseplate is dissipated by a laser beam, influenced by radiation and conduction. Gaussian profiles shown in Fig. 3 are used to represent the heat source per time. The time-dependent heat transfer phenomenon is expressed using the following equation (1) [11,14].

$$\rho C_{\rho\frac{\partial T}{\partial t}+\rho C_p u.\nabla T=\nabla.(k\nabla T)+Q} \quad (1)$$

where C is the heat capacity, T is the temperature, k is the thermal conductivity and t is the time. Q is the laser heat, ρ is the density and u is the velocity field which is calculated by the mass and momentum conservation equation.

The laser deposition process involves a body of heat load in the steel baseplate which is given by equation (2) [15].

$$Q(x,y,z) = SLaser(1-R_c).\frac{A_c}{\pi\sigma_x\sigma_y}e^{\frac{(x-x_0)^2}{2\sigma_x^2}+\frac{(y-y_0)^2}{2\sigma_y^2}}.e^{-A_c z} \quad (2)$$

The power input is represented by *SLaser*, the reflection coefficient is presented as R_c, the absorption coefficient is A_c while the Gaussian distribution along the XY-plane is represented in equation (3) [16].

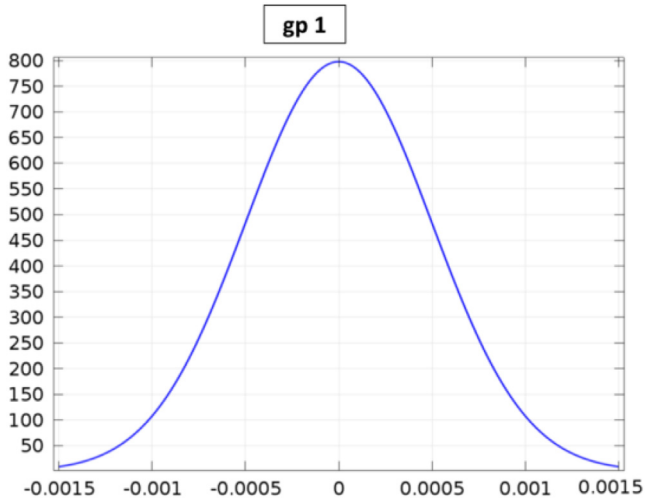

Fig. 3. Gaussian Profile.

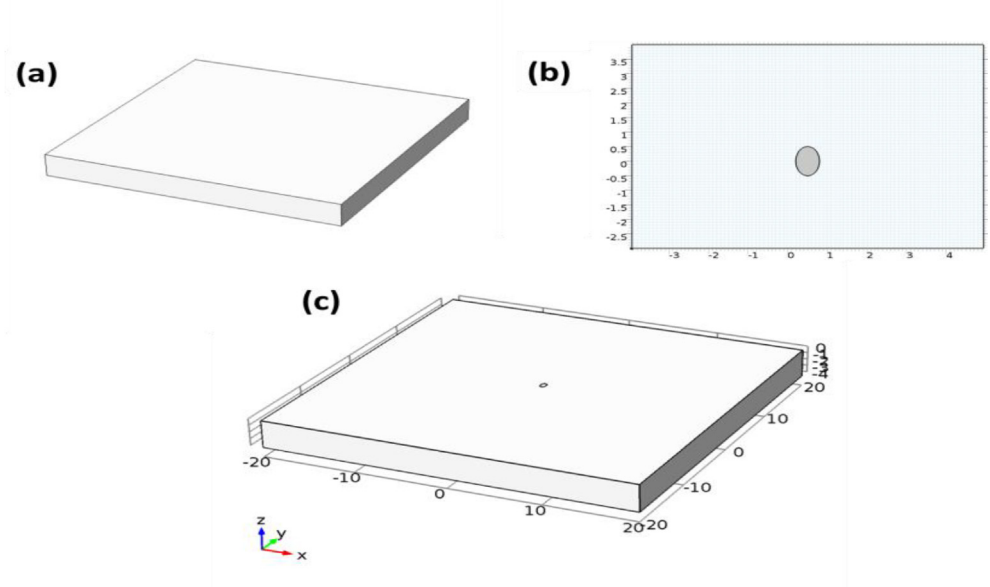

Fig. 2. (a) Base plate Geometry (b) The heat source (c) Geometry with the heat source.

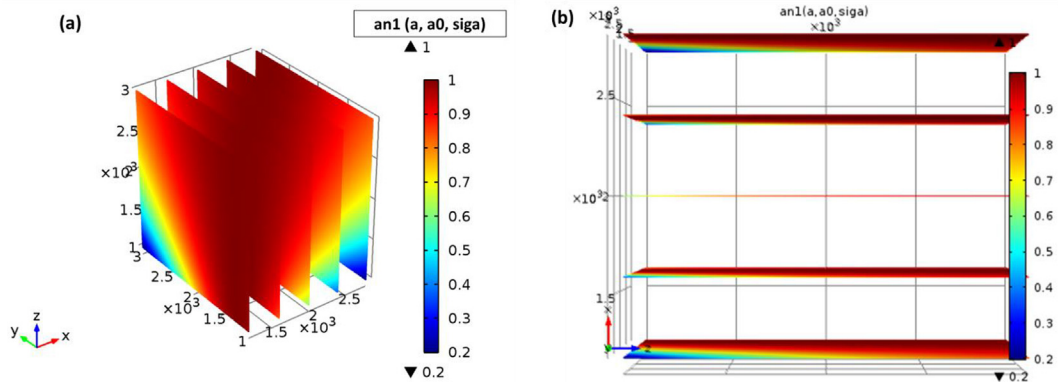

Fig. 4. Temperature Slice Plots of the Temperature Distribution.

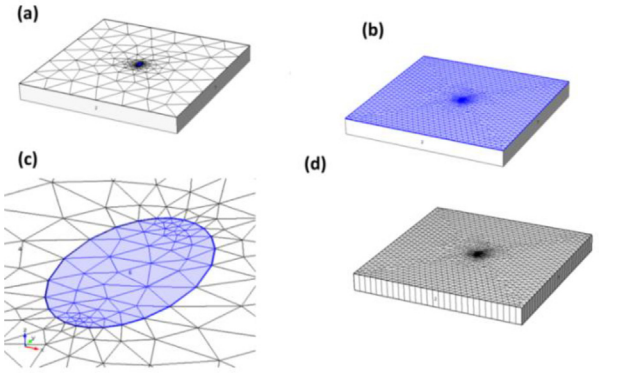

Fig. 5. Mesh (a) Coarse (b) Extra fine (c) Swept (d) 3D View of the baseplate with the mesh.

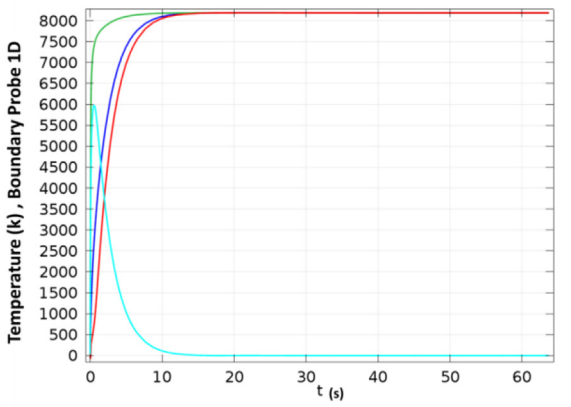

Fig. 6. Time-temperature Probe Plot.

$$e^{\frac{(x-x_0)^2}{2\sigma_x^2}+\frac{(y-y_0)^2}{2\sigma_y^2}} \tag{3}$$

While the exponential decay experienced due to absorption is given as $e^{-A_c z}$ since the planar surface is assumed to be aligned with z = 0.

3.2. Analytics

Name	Value
Expression	exp(-((a - a0)^2/(2*siga^2)))
Arguments	{a, a0, siga}
Arguments	mm, mm, mm
Function	3

3.3. Variables

Name	Expression	Description
Q_in	S_Laser *(1 - Rc)*Ac*(1/(pi*sigx*sigy))*an1(x, x0, sigx, y, y0, sigy)*exp(-Ac*abs(z))	Power input

3.4. Material parameters

Name	Value	Unit
Thermal conductivity	k(T[1/K])[W/(m*K)]	W/(m*K)
Heat capacity at constant pressure	C(T[1/K])[J/(kg*K)]	J/(kg*K)
Density	rho(T[1/K])[kg/m^3]	kg/m^3

3.5. Geometry

4. Heat flux

The laser heat source defined as the heat flux across the irradiated surface by the laser beam is the same size as the simulated laser beam which was distributed per time and represented using the Gaussian profile in Fig. 3. While the slice plots of the temperature distribution is shown in Fig. 4. The mathematical function is explained using the heat conduction volume equation (4) [17].

$$\rho C_p \frac{\partial T}{\partial t} - \nabla(k\nabla T) = Gt \tag{4}$$

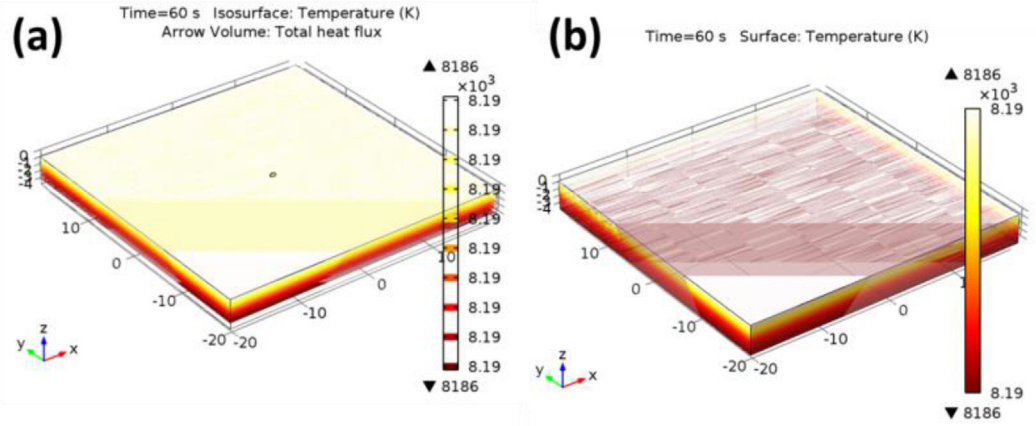

Fig. 7. Temperature Distribution Plot.

where the density of the steel is ρ, C_p is the specific heat capacity, k is the thermal conductivity, t is the time, T is the temperature The heat conduction shows the transfer from hot to the cold area inside the steel baseplate without macroscopic displacements or consideration of the work done by pressure changes and the viscous dissipation. The conduction occurred through the diffusion of free electrons in the steel when the surface is heated up and then the heat spreads in different directions towards the hemispherical melt pool shape with no significant deformation of the geometry.

4.1. Analytic

4.2. Mesh

The mesh phenomenon happens along the track, therefore the domain where the laser beam moves is meshed finer than other parts of the geometry to gain accuracy of the model. The mesh refinement was manually computed to re-compute solutions until no significant difference is observed between results with progressively finer elements. The minimum element size was valued at 2.8 while the maximum element size was at 20 with a resolution of 0.1 narrow regions and a growth rate of 2 in the extremely coarse mesh. Of Fig. 5 (a) and (C) while the extra fine mesh of Fig. 5 (b) and (d) had a minimum element size of 0.06 with a curvature factor of 0.3, a resolution of narrow region valued at 0.85 and 1.35 maximum element growth rate. The time–temperature profiles of the laser beam, indicating that the maximum temperature was achieved in 60 s is shown in Fig. 6 while the temperature distribution on the isothermal baseplate surface is shown in Fig. 7.

5. Conclusions

Comsol Multiphysics 4.4 was used to create a 2D transient heat transfer time-dependent model to simulate the temperature distribution on a HEA baseplate surface and determine the effect of temperature on the optimization process of the alloys. The temperature dependent model was developed by incorporating the material properties of the steel baseplate in different conditions with the temperature behaviour as the output parameter.

Gaussian profiles were used as the heat source distributed per time. The results showed the temperature distribution and the heat transfer presented in terms of thermal fields and Gaussian temperature profiles showed that the surface temperature distribution on the steel baseplate was sufficient enough to have a significant influence on the laser additive manufacturing technique improving adhesion and reduce thermal stresses thus, facilitating the optimization process of the HEA. The objective of the simulation was to observe the influence of temperature distribution on the optimization process and the model was helpful to define the range of temperature optimization could be achieved. More studies should be carried out to investigate the melting kinetics at higher temperature ranges. Simulation modelling is a significant tool in the optimization of laser additive process parameters as it was observed that as the preheating temperature at 400 °C was applied on the surface of the baseplate, the stresses decreased during fabrication resulting in the production of quality clads.

Declaration of Competing Interest

The authors declare that they have no known competing financial interests or personal relationships that could have appeared to influence the work reported in this paper.

Acknowledgments

The authors will like to appreciate Prof. Sisa Pityana at the Council for Scientific and Industrial Research (CSIR), the National Laser Center (Laser Enabled Manufacturing Resource Group), Juwon Ojo Fayomi and Uyor Uwa Orji at the Surface Engineering Research Laboratory (SERL), Tshwane University of Technology, Pretoria, South Africa for their technical support during this research.

References

[1] D.D. Gu et al., Laser additive manufacturing of metallic components: materials, processes and mechanisms, Int. Mater. Rev. 57 (3) (2012) 133–164.
[2] D. Gu, Laser Additive Manufacturing of High-Performance Materials, Springer, 2015.
[3] M. Dada et al., Fabrication and hardness behaviour of high entropy alloys, TMS 2020 149th Annual Meeting & Exhibition Supplemental Proceedings, Springer, 2020.
[4] M. Dada et al., Process optimization of high entropy alloys by laser additive manufacturing, Eng. Rep. 2 (10) (2020) e12252.
[5] O. Fergani et al., Analytical modelling of residual stress in additive manufacturing, Fatigue Fract. Eng. Mater. Struct. 40 (6) (2017) 971–978.
[6] G. Farotade et al., Computational analysis of heat transfer within a Ti-6Al-4V alloy substrate during laser cladding process, Mater. Res. Express 6 (4) (2019) 046516.
[7] N. Bianco et al., A numerical model for transient heat conduction in semi-infinite solids irradiated by a moving heat source, Proceedings of the COMSOL Conference, 2008.
[8] H.L. Oo, Optimization of a parameter in laser heating process.
[9] M. Darif, N. Semmar, F. Orléans Cedex, Numerical simulation of Si nanosecond laser annealing by COMSOL multiphysics, Proceedings of the COMSOL Conference 2008 Hannover, 2008.
[10] F. Caiazzo, V. Alfieri, Simulation of laser heating of aluminum and model validation via two-color pyrometer and shape assessment, Materials 11 (9) (2018) 1506.

[11] R. Parekh, R.K. Buddu, R. Patel, Multiphysics simulation of laser cladding process to study the effect of process parameters on clad geometry, Procedia Technol. 23 (2016) 529–536.
[12] S. Morville et al., Numerical modeling of powder flow during coaxial laser direct metal deposition–comparison between Ti-6Al-4V alloy and stainless steel 316L, Proceedings of the 2012 COMSOL Conference, 2012.
[13] Z. Cao et al., Temperature field in the heat transfer process of PEEK thermoplastic composite fiber placement, Materials 13 (19) (2020) 4417.
[14] B.K. Panda, S. Sarkar, A.K. Nath, 2D thermal model of laser cladding process of Inconel 718, Mater. Today: Proc. 41 (2021) 286–291.
[15] S. Camosso, Gaussian integrals depending by a quantum parameter in finite dimension. arXiv preprint arXiv:2107.06874, 2021.
[16] G. Georgieva-Tsaneva, Simulation of long-term Heart Rate Variability records with Gaussian distribution functions, International Conference on Computer Systems and Technologies' 21, 2021.
[17] A.N. Bakhtiyari et al., A review on applications of artificial intelligence in modeling and optimization of laser beam machining, Opt. Laser Technol. 135 (2021) 106721.